

Initial highlights of the HOBYS key program, the Herschel imaging survey of OB young stellar objects

F. Motte, Annie Zavagno, Sylvain Bontemps, N. Schneider, M. Hennemann, J. Di Francesco, Ph. André, P. Saraceno, M. Griffin, A. Marston, et al.

▶ **To cite this version:**

F. Motte, Annie Zavagno, Sylvain Bontemps, N. Schneider, M. Hennemann, et al.. Initial highlights of the HOBYS key program, the Herschel imaging survey of OB young stellar objects. Astronomy and Astrophysics - A&A, 2010, 518, pp.L77. 10.1051/0004-6361/201014690 . hal-00526246

HAL Id: hal-00526246
https://hal.science/hal-00526246

Submitted on 1 Dec 2021

HAL is a multi-disciplinary open access archive for the deposit and dissemination of scientific research documents, whether they are published or not. The documents may come from teaching and research institutions in France or abroad, or from public or private research centers.

L'archive ouverte pluridisciplinaire **HAL**, est destinée au dépôt et à la diffusion de documents scientifiques de niveau recherche, publiés ou non, émanant des établissements d'enseignement et de recherche français ou étrangers, des laboratoires publics ou privés.



Distributed under a Creative Commons Attribution 4.0 International License

A&A 518, L77 (2010)
DOI: 10.1051/0004-6361/201014690
© ESO 2010

Astronomy & Astrophysics
Special feature

Herschel: the first science highlights

Letter to the Editor

Initial highlights of the HOBYS key program, the *Herschel*⋆ imaging survey of OB young stellar objects⋆⋆

F. Motte[1], A. Zavagno[2], S. Bontemps[1,3], N. Schneider[1], M. Hennemann[1], J. Di Francesco[4], Ph. André[1], P. Saraceno[5], M. Griffin[6], A. Marston[7], D. Ward-Thompson[6], G. White[8,9], V. Minier[1], A. Men'shchikov[1], T. Hill[1], A. Abergel[10], L. D. Anderson[2], H. Aussel[1], Z. Balog[11], J.-P. Baluteau[2], J.-Ph. Bernard[12], P. Cox[13], T. Csengeri[1], L. Deharveng[2], P. Didelon[1], A.-M. di Giorgio[5], P. Hargrave[6], M. Huang[14], J. Kirk[6], S. Leeks[8], J. Z. Li[14], P. Martin[15], S. Molinari[5], Q. Nguyen-Luong[1], G. Olofsson[16], P. Persi[17], N. Peretto[1], S. Pezzuto[5], H. Roussel[18], D. Russeil[2], S. Sadavoy[4], M. Sauvage[1], B. Sibthorpe[19], L. Spinoglio[5], L. Testi[20], D. Teyssier[7], R. Vavrek[7], C. D. Wilson[21], and A. Woodcraft[19]

(Affiliations are available in the online edition)

Received 31 March 2010 / Accepted 12 May 2010

ABSTRACT

We present the initial highlights of the HOBYS key program, which are based on *Herschel* images of the Rosette molecular complex and maps of the RCW120 H II region. Using both SPIRE at 250/350/500 μm and PACS at 70/160 μm or 100/160 μm, the HOBYS survey provides an unbiased and complete census of intermediate- to high-mass young stellar objects, some of which are not detected by *Spitzer*. Key core properties, such as bolometric luminosity and mass (as derived from spectral energy distributions), are used to constrain their evolutionary stages. We identify a handful of high-mass prestellar cores and show that their lifetimes could be shorter in the Rosette molecular complex than in nearby low-mass star-forming regions. We also quantify the impact of expanding H II regions on the star formation process acting in both Rosette and RCW 120.

Key words. stars: formation – stars: massive – telescopes – stars: protostars – H II regions – dust, extinction

1. Introduction and first constraints from HOBYS

Our knowledge of high-mass (OB, $M_\star > 8\ M_\odot$) star formation is still rather schematic, but an evolutionary sequence of their earliest phases is starting to emerge. Bright *IRAS* sources embedded within massive envelopes have been recognized as HMPOs containing evolved high-mass protostars (e.g. Beuther et al. 2002). Cold massive dense cores associated with weak mid-infrared emission, but with clear signposts of OB-type protostars, have been qualified as IR-quiet and observed to harbor high-mass class 0 protostars (Motte et al. 2007; Bontemps et al. 2010b). Controversy remains about the existence and the lifetime of high-mass analogs of prestellar cores, since infrared dark clouds are numerous (Simon et al. 2006) but only a few harbor starless, massive, and dense enough cores (e.g. Motte et al. 2007). Large surveys covering the far-infrared to (sub)millimeter continuum regime are required to improve the statistics of present studies and constrain models proposed for the formation of high-mass stars (e.g. Krumholz et al. 2007; Bonnell & Bate 2006).

The "*Herschel* imaging survey of OB Young Stellar objects" (HOBYS, see http://hobys-herschel.cea.fr) is a guaranteed time key program jointly proposed by the SPIRE and PACS consortia, and the Herschel Science Centre. It will use the SPIRE and PACS cameras (Griffin et al. 2010; Poglitsch et al. 2010) of the *Herschel* satellite (Pilbratt et al. 2010) to image essentially all of the regions forming OB-type stars at distances less than 3 kpc from the Sun. The 70/160 μm or 100/160 μm PACS and 250/350/500 μm SPIRE images from HOBYS will provide an unbiased census of massive young stellar objects (YSOs) and trace the large-scale emission of the surrounding clouds. This survey will yield, for the first time, accurate bolometric luminosity and envelope mass estimates for homogeneous and complete samples of OB-type YSOs. It will also reveal spatial variations in the cloud temperature and assist in quantifying the importance of external triggers in the star formation process.

The Rosette molecular complex and the RCW 120 H II region were selected as targets for the science demonstration phase. Of the 9 high-mass star-forming regions in HOBYS, the Rosette molecular cloud ($2 \times 10^5\ M_\odot$, 1.6 kpc away) is well-known for its interaction with an expanding H II region powered by the OB cluster NGC 2244. Among the first results, (1) Schneider et al. (2010) measure a clear dust temperature gradient and a potential age gradient of YSOs through the Rosette molecular cloud; (2) Di Francesco et al. (2010) show that the mass spectrum of Rosette clumps is different from the stellar initial mass function; (3) Hennemann et al. (2010) constrain the evolutionary stage of low- to high-mass protostars revealed in Rosette. Located only 1.3 kpc away, RCW 120 is a bubble-shaped H II region at the periphery of which triggered star formation has been clearly established. Among the first results of HOBYS, Zavagno et al. (2010) identify, in RCW 120, the first massive class 0 protostar formed by means of the collect and collapse process.

2. *Herschel* observations

The Rosette molecular cloud was observed on October 20, 2009 using the parallel mode with a scanning speed of 20″/s

⋆ *Herschel* is an ESA space observatory with science instruments provided by European-led Principal Investigator consortia and with important participation from NASA.

⋆⋆ Figures 4 and 5 are only available in electronic form at http://www.aanda.org



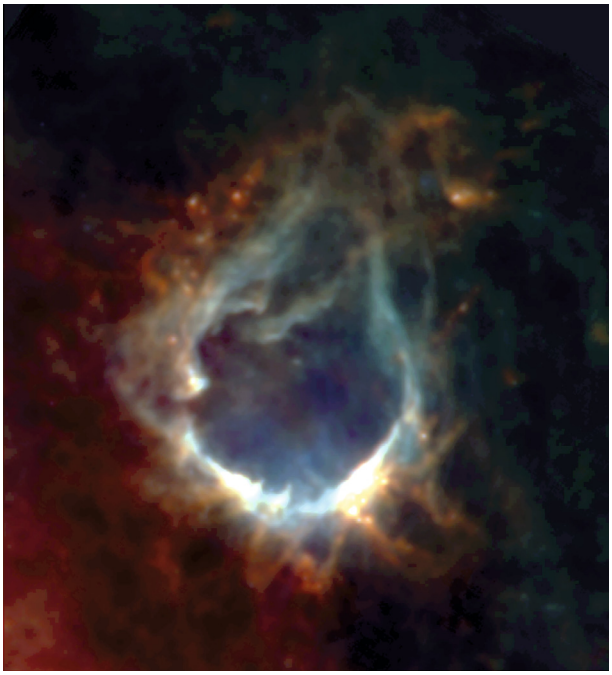


Fig. 1. Composite 3-color *Herschel* images of the Rosette molecular complex (**a**), *left*) and the RCW 120 H II region (**b**), *right*): PACS 70 μm for the Rosette and 100 μm for RCW 120 (blue), PACS 160 μm (green), and SPIRE 250 μm (red). These maps were observed during the science demonstration phase of the HOBYS and Abergel et al. (2010) key programs. The images at each wavelength are presented in Figs. 4a–e and partly in Figs. 1, 2 of Zavagno et al. (2010).

simultaneously with SPIRE at 250/350/500 μm and PACS at 70/160 μm. The RCW 120 H II region was imaged on October 9, 2009 with PACS at 100/160 μm and on September 12, 2009 with SPIRE at 250/350/500 μm, using a scanning speed of 30″/s. The data reduction is described in Schneider et al. (2010), Hennemann et al. (2010), and Zavagno et al. (2010).

Figures 1a, b present three-color (blue: 70 or 100 μm / green: 160 μm / red: 250 μm) images of the Rosette molecular complex and the RCW 120 H II region. The sensitivities achieved in these images allow detection of compact YSOs down to $5\sigma \simeq 0.3\ M_{\odot}$ at 160 μm. Noise measurements were taken in low-cirrus noise parts of the maps, and they correspond to several times the instrumental sensitivity for point sources (see caption of Fig. 4). The *Herschel* images of the Rosette molecular cloud are sensitive to spatial scales ranging from ~0.05–0.2 pc (corresponding to a resolution of ~6″–25″) to ~40 pc (i.e., the ~1.5° spatial filter used for data reduction). The resulting spatial dynamic range of SPIRE images (~200) is 4 times greater than for ground-based submillimeter observations with the best spatial dynamics (e.g. Motte et al. 2007 with MAMBO-2). PACS images display an unmatched angular resolution at far-infrared wavelengths (down to ~6″ at 70 μm) and have a spatial dynamic range up to 1000.

3. Massive dense cores in the Rosette complex

Our main goal is to investigate potential sites of star formation, we thus focus here on small-scale (~0.1 pc) dense cloud fragments. We applied a source extraction technique based on a multi-resolution analysis (Motte et al. 2007). We filtered out the spatial scales larger than 0.5 pc using the *MRE* algorithm (Starck & Murtagh 2006) and applied the *GaussCLumps* program (Kramer et al. 1998) to each *Herschel* image independently. Above the 5σ level given in Fig. 4, this method identifies ~4000 to ~900 sources at 70 μm and 500 μm, respectively. The individual catalogs from each of the 5 wavebands were cross-linked with the TopCat tool allowing offsets of one half-beam size (i.e. 6″ to 20″) from the PACS 70 μm positions for sources identified at 160–500 μm. Slightly larger offsets were used for starless dense cores to account for their emission generally being less centrally peaked.

Our analysis in the Rosette yields an *MRE-GCL* catalog of dense cores with sizes 0.02–0.3 pc at 160 μm (see Fig. 5a) and fluxes measured in most, if not all, *Herschel* wavebands. Given a range of six across the angular resolution of the *Herschel* images, the source extraction technique tended to measure larger (deconvolved) sizes at 500 μm than at 160 μm. Such behavior is found in radiative transfer modeling of protostellar envelopes: the colder the dust dominating at 500 μm, the farther away the emission from the heating protostar. However, this observed effect is strong for both pre- and protostellar dense cores and is stronger in clustered environments. This size-wavelength relation is thus most likely related to the classical distribution of gas under the influence of gravity observed with optically-thin column density tracers (Motte & André 2001; Beuther et al. 2002)[1]. In order to keep the best of the PACS angular resolution, we define here the nominal size of dense cores as the deconvolved *FWHM* size derived from a 2D-Gaussian fit to the 160 μm image. We then scaled down the SPIRE 250 μm, 350 μm, and 500 μm integrated fluxes measured for these dense cores assuming the $S_{\lambda}(< r) \propto r$ relation.

[1] Protostellar envelopes and the outer part of prestellar cores with $\rho(r) \propto r^{-1.5} - r^{-2}$ and $T_{\rm dust}(r) \propto r^{-0.4} - r^{0}$ distributions display optically thin emission with intensity laws close to $S_{\lambda}(<r) \propto r$.

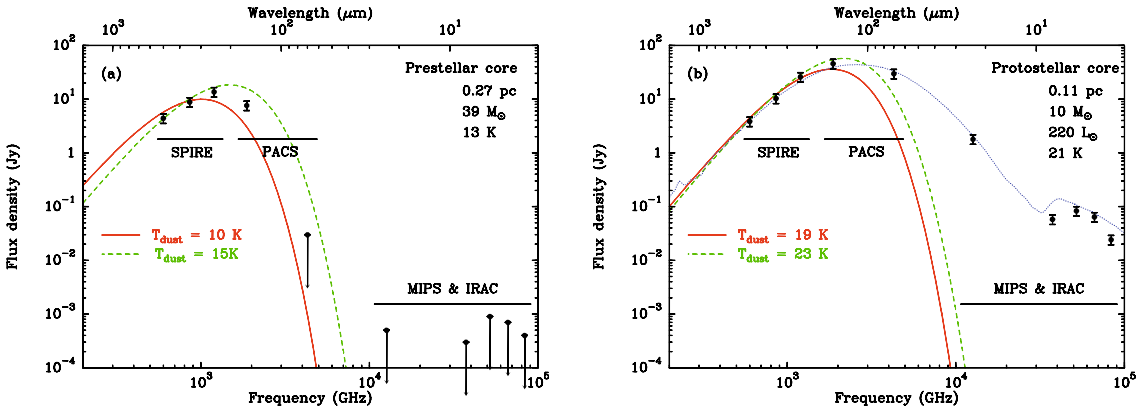


Fig. 2. SEDs built from *Herschel* and *Spitzer* fluxes of: **a)** one massive prestellar core and **b)** one intermediate-mass protostellar dense core. Their submillimeter components are compared to graybody models, while a model by Robitaille et al. (2007) is fitted to the complete SED of **b)**.

We computed SEDs for the 46 most massive dense cores using the aforementioned *Herschel* fluxes and the *Spitzer*/MIPS and IRAC fluxes of Balog et al. (in. prep.) (see Figs. 2a, b). The mass of each dense core was determined by fitting simple graybody models to the submillimeter component of their SED (i.e. 4 observed fluxes from 500 μm to 160 μm). From the ground, a single submillimeter flux and a pre-defined dust temperature are generally taken but *Herschel* provides the unique opportunity to directly measure the mass-averaged dust temperature and the mass of each dense core. We determine a temperature varying from 12 to 40 K and a mass from 0.8 $M_\odot$ to 39 $M_\odot$ (see Fig. 5a), assuming a dust opacity per unit (gas + dust) mass of $\kappa_\nu = 0.1$ cm^2 g^{-1} $\times$ (ν/1000 GHz)^2. No measurement longward of 500 μm can currently constrain the emissivity index (β) that was set to 2. While graybodies are the correct models for fitting starless dense cores and the outer cold part of protostellar envelopes, they fail to fit fluxes measured at 70 μm and shorter (e.g. Fig. 2b). More complex radiative transfer modeling, such as those proposed by Robitaille et al. (2007), are needed to estimate other protostellar characteristics, such as the mass and luminosity of the stellar embryo. However, this is not within the scope of this paper. The bolometric luminosity of each massive dense core was estimated by integrating their fluxes below the SED from 500 μm to 3.6 μm.

The starless or protostellar nature of the dense cores in Rosette was determined by searching for pointlike *Spitzer* 24 μm sources, which lie within the *Herschel* dense cores (see Balog et al. in prep. and Poulton et al. 2008). We followed the definition by Motte et al. (2007) for the massive ($\gtrsim$20 $M_\odot$) dense cores harboring high-mass protostars. They are qualified as IR-quiet (i.e. young, and have accreted less than 8 $M_\odot$) and IR-bright (i.e. more evolved) when they have a bolometric luminosity that is lower or respectively higher than 10^3 $L_\odot$, corresponding to that of a B3 star on the main sequence.

4. Discussion and conclusion

The HOBYS program was designed to essentially survey all of the massive star-forming complexes out to 3 kpc. Integrating the estimated star formation rate in the Galactic disk (McKee & Williams 1997) within a volume of a 3 kpc radius suggests a star formation rate of ~0.2 $M_\odot$/yr in the selected molecular cloud complexes. With such an estimate, and assuming a standard initial mass function (Kroupa 2001) and a lifetime of 1×10^5 yr (Motte et al. 2007; Russeil et al. 2010), the HOBYS survey should reveal about 250 high-mass protostars (from IR-quiet to IR-bright).

Given the mass of the Rosette molecular complex, and assuming a similar star formation efficiency for all the HOBYS clouds, we expect ~5 high-mass protostars in the *Herschel* image of Rosette. Above 19 $M_\odot$ (the limit set to encompass all the massive IR-bright dense cores), we identified 6 protostellar and 3 prestellar dense cores with radii ~0.18 pc and masses between ~20–40 $M_\odot$ (see Figs. 5a–c).

4.1. High-mass protostellar dense cores

The two most luminous of these sources, AFGL 961 and IRAS 06308+0402 (see Fig. 5c), have a mass of ~22 $M_\odot$ and luminosity of ~1$\times$ and 4×10^3 $L_\odot$. They correspond to two luminous *IRAS* point sources previously identified by Cox et al. (1990) as precursors of OB stars. From the mass and luminosity derived by these *Herschel* observations, they are classified as IR-bright, high-mass protostellar dense cores (see Sect. 3).

Four other protostellar dense cores are as massive as these IR-bright dense cores, but they are far less luminous ~15–75 $L_\odot$ and cooler at 15 K (compared with 29 K). They are therefore good candidates for hosting early stage, high-mass protostars, although follow-up observations in search of powerful outflows, hot cores, and/or maser emission are needed to ascertain their nature. Higher resolution studies of these massive protostellar dense cores confirm that the majority of them are dominated, in terms of both mass and luminosity, by a single massive protostar (Williams et al. 2009; Hennemann et al. 2010).

4.2. Discovery of intermediate-/high-mass prestellar cores

We detected three massive starless cores with slightly larger sizes and higher masses (~0.22 pc, ~30 $M_\odot$) and with cooler temperatures (13 K, see Fig. 2a) than for protostellar cores. Given their high densities (~10^5 cm^{-3}) and cooler temperatures, they probably are gravitationally bound and represent the high-mass analog of low-mass prestellar cores. These three objects are among the first massive prestellar cores, since virtually none have been detected in surveys of the Cygnus X and NGC 6334 complexes (Motte et al. 2007; Russeil et al. 2010).

A handful of starless dense cores were also discovered to have warm temperatures: ~1–9 $M_\odot$, ~0.14 pc, ~27 K (see Fig. 5a). The nature of these objects is as yet unclear, but they do not seem to correspond to remnant cloud surrounding an already formed cluster. If gravitationally bound, these warm, massive, but not centrally peaked, dense cores could concentrate their mass, cool down, and then form the next generation of intermediate- to high-mass stars in the Rosette. They have high

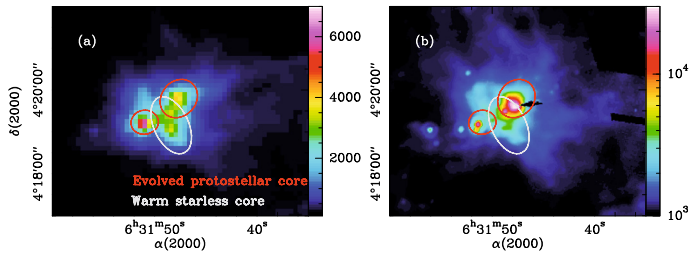


Fig. 3. **a)** *Herschel*/PACS 160 μm and **b)** *Spitzer*/MIPS 24 μm images of the bright *IRAS* source associated to the PL1 embedded cluster. Ellipses outline the 2×*FWHM* size of dense cores.

luminosities (~100 $L_\odot$) and are part of the >10^3 $L_\odot$ *IRAS* point sources associated with the PL1, PL3, and PL4 embedded clusters (see Fig. 5c and Cox et al. 1990). With the higher spatial resolution of PACS images, these *IRAS* sources are resolved into small clusters containing intermediate-mass evolved protostars and warm starless cores (see e.g. Fig. 3).

4.3. Evolutionary sequence and lifetime of YSOs

One of the main goals of the HOBYS survey is to better constrain the evolutionary sequence of OB-type YSOs and the lifetimes of massive prestellar cores and protostars. Our analysis in the Rosette molecular cloud is extendable to progenitors of intermediate-mass stars. The sample of dense cores shown in Figs. 5a, b is complete down to ~8 $M_\odot$ and contains 31 objects more massive than this limit. With the criteria given in Sect. 3, we identify 8 dense cores as prestellar and 22 as protostellar. We used the mass-luminosity diagram and mass-averaged temperature of protostellar dense cores as evolutionary indicators. In Fig. 5b, YSOs should statistically evolve from the top-left to the bottom-right since the envelope material is accreted onto the protostar that gets more luminous. This trend is in overall agreement with the rise in envelope temperature expected during the protostellar accretion. We used the $M \propto L^{0.6}$ linear relation found for low-mass protostars (cf. Bontemps et al. 2010a) to draw a boundary zone between $14\pm^1_3$ "young" and $8\pm^3_1$ "evolved" protostellar dense cores. Given the low-level statistics, the relative number of prestellar cores, young protostars, and evolved protostars is very similar for this intermediate- to high-mass range.

If we assume that the protostellar lifetime equals the free-fall time of these dense cores, we derive a statistical lifetime of $\sim 8 \times 10^4$ yr for the prestellar phase of intermediate-mass star formation. Such a result suggests that the lifetime of prestellar cores in Rosette is a few times shorter than found in nearby low-mass star-forming regions (Kirk et al. 2005, $1-4 \times 10^5$ yr), and a few times longer than measured in high-mass star-forming complexes (Motte et al. 2007; Russeil et al. 2010, $3-9 \times 10^4$ yr). If confirmed, this result could suggest either that the prestellar lifetime depends on the final mass of the star that they will form or that statistical lifetimes cannot be used since star formation often proceeds in bursts.

4.4. Triggered star formation

The *Herschel* images of both the Rosette molecular cloud and the Galactic ionized region RCW 120 display clear dust temperature gradients from 10 to 30 K (Schneider et al. 2010; Anderson et al. 2010). The spatial scales affected are, however, quantitatively different (30 pc versus 0.5 pc) and in probable relation to the presence of an OB cluster rather than a single ionizing source. These gradients are observed at densities up to ~10^5 cm^{-3}, thus demonstrating the strong influence of H II regions on their associated cloud. The spatial distribution of the most massive YSOs in the Rosette also supports a possible age gradient from OB stars to evolved protostars and finally to young protostars and prestellar cores (Schneider et al. 2010). The HOBYS survey will be able to constrain the star formation history of isolated template regions, such as the RCW 120 H II region, and more common star-forming regions, such as the Rosette, providing the means to estimate the efficiency of triggered star formation in regular high-mass star-forming complexes.

Promising results have been obtained during the science demonstration phase of the *Herschel* key program HOBYS. They show how strongly the complete HOBYS survey will deepen our understanding of the high-mass star formation process, especially during the earliest phases.

Acknowledgements. SPIRE has been developed by a consortium of institutes led by Cardiff Univ. (UK) and including Univ. Lethbridge (Canada); NAOC (China); CEA, LAM (France); IFSI, Univ. Padua (Italy); IAC (Spain); Stockholm Observatory (Sweden); Imperial College London, RAL, UCL-MSSL, UKATC, Univ. Sussex (UK); Caltech, JPL, NHSC, Univ. Colorado (USA). This development has been supported by national funding agencies: CSA (Canada); NAOC (China); CEA, CNES, CNRS 7(France); ASI (Italy); MCINN (Spain); SNSB (Sweden); STFC (UK); and NASA (USA). PACS has been developed by a consortium of institutes led by MPE (Germany) and including UVIE (Austria); KU Leuven, CSL, IMEC (Belgium); CEA, LAM (France); MPIA (Germany); INAF-IFSI/OAA/OAP/OAT, LENS, SISSA (Italy); IAC (Spain). This development has been supported by the funding agencies BMVIT (Austria), ESA-PRODEX (Belgium), CEA/CNES (France), DLR (Germany), ASI/INAF (Italy), and CICYT/MCYT (Spain). Part of this work was supported by the ANR (*Agence Nationale pour la Recherche*) project "PROBeS", number ANR-08-BLAN-0241.

References

Abergel, A., et al. 2010, A&A, 518, L96
Anderson, L. D., et al. 2010, A&A, 518, L99
Beuther, H., Schilke, P., Menten, K. M., et al. 2002, ApJ, 566, 945
Bonnell, I., & Bate, M. 2006, MNRAS, 370, 488
Bontemps, S., et al. 2010a, A&A, 518, L85
Bontemps, S., Motte, F., Csengeri, T., & Schneider, N. 2010b, A&A, submitted
Cox, P., Deharveng, L., & Leene, A. 1990, A&A, 230, 181
Di Francesco, J., et al., 2010, A&A, 518, L91
Griffin, M. J., et al. 2010, A&A, 518, L3
Hennemann, M., et al., 2010, A&A, 518, L84
Kirk, J. M., Ward-Thompson, D., & André, P. 2005, MNRAS, 360, 1506
Kramer, C., Stutzki, J., Rohrig, R., & Corneliussen, U. 1998, A&A, 329, 249
Kroupa, P. 2001, MNRAS, 322, 231
Krumholz, M. R., Klein, R. I., & McKee, C. F. 2007, ApJ, 656, 959
McKee, C. F., & Williams, J. P. 1997, ApJ, 476, 144
Motte, F., & André, P. 2001, A&A, 365, 440
Motte, F., Bontemps, S., Schilke, P., et al. 2007, A&A, 476, 1243
Pilbratt, G. L., et al. 2010, A&A, 518, L1
Poglitsch, A., et al. 2010, A&A, 518, L2
Poulton, C. J., Robitaille, T. P., Greaves, J. S., et al. 2008, MNRAS, 384, 1249
Robitaille, T. P., Whitney, B. A., Indebetouw, R., & Wood, K. 2007, ApJS, 169, 328
Russeil, D., Zavagno, A., Motte, F., et al. 2010, A&A, 515, A55
Schneider, N., et al. 2010, A&A, 518, L83
Simon, R., Rathborne, J. M., Shah, R. Y., Jackson, J. M., & Chambers, E. T. 2006, ApJ, 653, 1325
Starck, J.-L., & Murtagh, F. 2006, Astronomical image and data analysis (Berlin: Springer), Astronomy and astrophysics library
Williams, J. P., Mann, R. K., Beaumont, C. N., et al. 2009, ApJ, 699, 1300
Zavagno, A., Russeil, D., Motte, F., et al. 2010, A&A, 518, L81

Pages 5 to 6 are available in the electronic edition of the journal at http://www.aanda.org

[1] Laboratoire AIM, CEA/IRFU – CNRS/INSU – Université Paris Diderot, CEA-Saclay, 91191 Gif-sur-Yvette Cedex, France
e-mail: frederique.motte@cea.fr
[2] Laboratoire d'Astrophysique de Marseille, CNRS/INSU – Université de Provence, 13388 Marseille Cedex 13, France
e-mail: annie.zavagno@oamp.fr
[3] Laboratoire d'Astrophysique de Bordeaux, CNRS/INSU – Université de Bordeaux, BP 89, 33271 Floirac cedex, France
e-mail: bontemps@obs.u-bordeaux1.fr
[4] National Research Council of Canada, Herzberg Institute of Astrophysics, University of Victoria, Department of Physics and Astronomy
[5] Istituto di Fisica dello Spazio Interplanetario, INAF, via del Fosso del Cavaliere 100, 00133 Roma, Italy
[6] School of Physics & Astronomy, Cardiff University, Queens Buildings The Parade, Cardiff CF24 3AA, UK
[7] Herschel Science Centre, ESAC, ESA, PO Box 78, Villanueva de la Cañada, 28691 Madrid, Spain
[8] Space Science and Technology Department, Rutherford Appleton Laboratory, Didcot, Oxon OX11 0QX, UK
[9] Department of Physics & Astronomy, The Open University, Milton Keynes MK7 6AA, UK
[10] IAS, Université Paris-Sud, 91435 Orsay, France
[11] Max-Planck-Institut für Astronomie, Königstuhl 17, Heidelberg, Germany
[12] CESR & UMR 5187 du CNRS/Université de Toulouse, BP 4346, 31028 Toulouse Cedex 4, France
[13] IRAM, 300 rue de la Piscine, Domaine Universitaire, 38406 Saint Martin d'Hères, France
[14] National Astronomical Observatories, Chinese Academy of Sciences, Beijing 100012, PR China
[15] CITA & Dep. of Astronomy and Astrophysics, University of Toronto, Toronto, Canada
[16] Department of Astronomy, Stockholm University, AlbaNova University Center, Roslagstullsbacken 21, 10691 Stockholm, Sweden
[17] INAF-IASF, Sez. di Roma, via Fosso del Cavaliere 100, 00133 Roma, Italy
[18] Institut d'Astrophysique de Paris, Université Pierre & Marie Curie, 98bis boulevard Arago, 75014 Paris, France
[19] UK Astronomy Technology Centre, Royal Observatory Edinburgh, Blackford Hill EH9 3HJ, UK
[20] ESO, Karl Schwarzschild Str. 2, 85748, Garching, Germany
[21] Dept. of Physics & Astronomy, McMaster University, Hamilton, Ontario, L8S 4M1, Canada

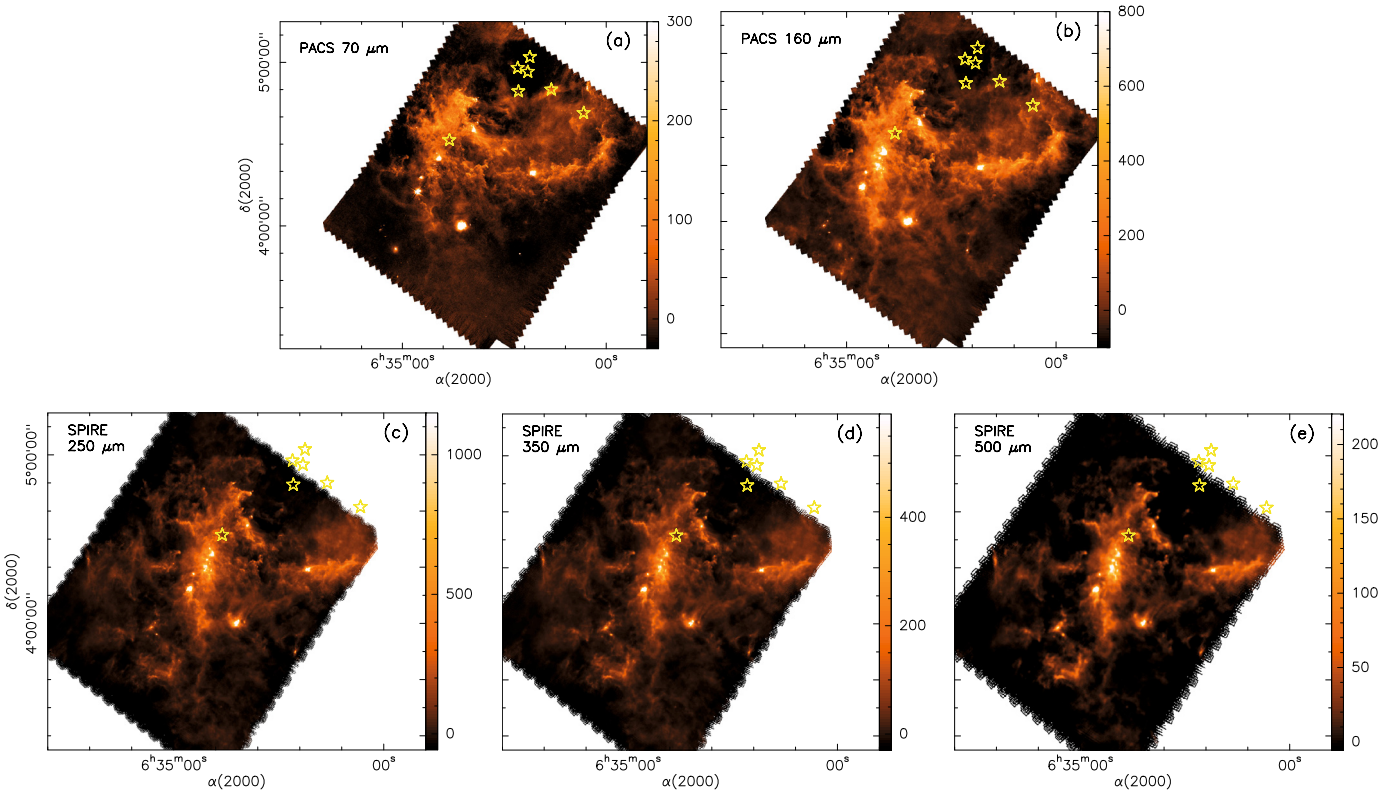


Fig. 4. *Herschel* far-infrared to submillimeter images of the Rosette molecular complex: **a)** PACS 70 μm with angular resolution and rms of $HBPW \simeq 5.5'' \times 6.5''$ and $1\sigma \simeq 6$ MJy/sr; **b)** PACS 160 μm with $HBPW \simeq 10.7'' \times 13''$ and $1\sigma \simeq 5.5$ MJy/sr; **c)** SPIRE 250 μm with $HBPW \simeq 18.1''$ and $1\sigma \simeq 2.5$ MJy/sr; **d)** SPIRE 350 μm with $HBPW \simeq 25.2''$ and $1\sigma \simeq 1.2$ MJy/sr; **e)** SPIRE 500 μm with $HBPW \simeq 36.9''$ and $1\sigma \simeq 0.5$ MJy/sr. A common SPIRE/PACS area of $1° \times 1°$ is achieved with $1°45' \times 1°30'$ SPIRE and PACS images offsetted by ~23′. The images were flux-calibrated according to the correction factors of Griffin et al. (2010) and Poglitsch et al. (2010): /1.05 at 70 μm, /1.29 at 160 μm, ×1.02 at 250 μm, ×1.05 at 350 μm, and ×0.94 at 500 μm. The conversion to MJy/sr unit is done by multiplying the HIPE output images **a)–e)** by ~4150, ~1040, ~115, ~59.1, and ~27.6.

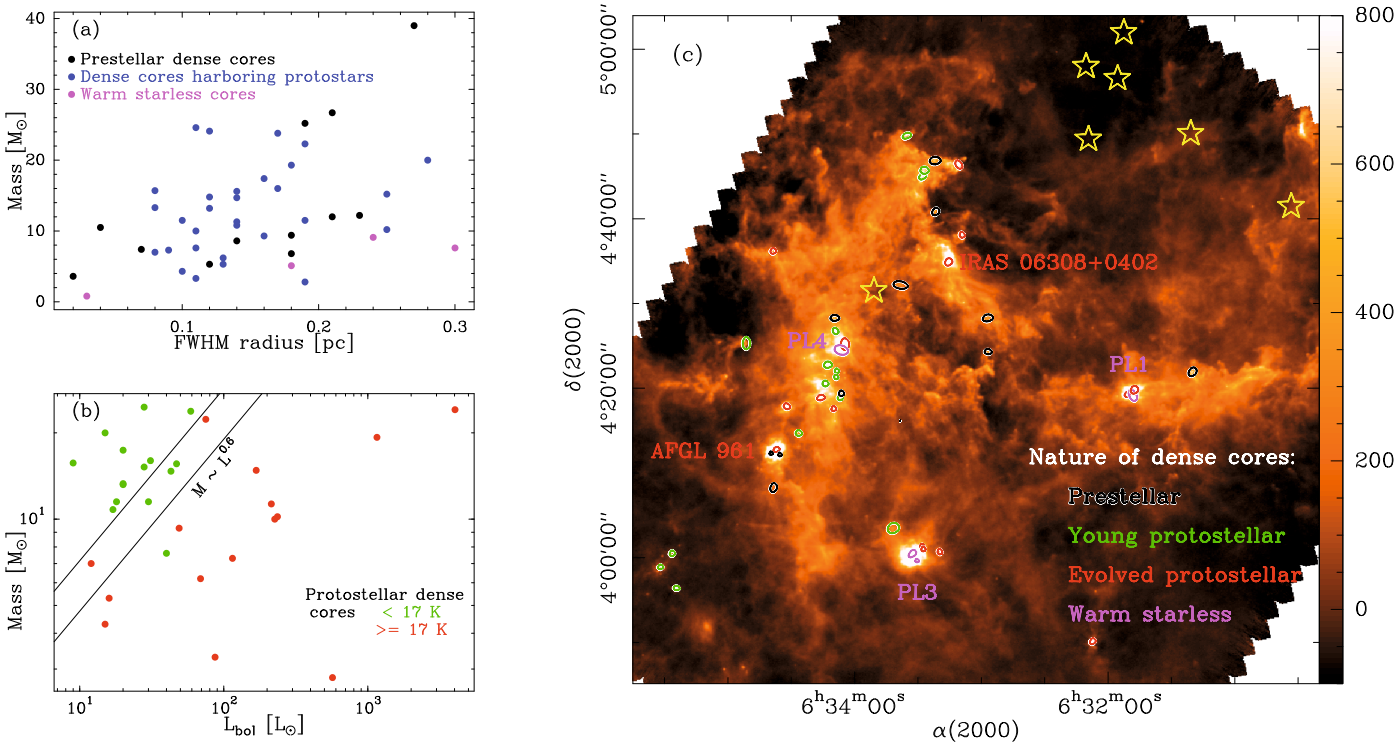


Fig. 5. The 46 most massive dense cores of the Rosette molecular cloud: **a)** mass-radius, **b)** mass-luminosity diagrams, and **c)** spatial distribution on the 160 μm map as a function of their estimated nature and evolutionary state. The OB cluster powering the NGC 2244 nebula is marked with stars and the five $>10^3$ $L_\odot$ *IRAS* sources are indicated in red and pink.